Scientific review of watershed and water quality modeling to support nutrient management in the Falls Lake watershed

Year 1 summary report (July 2020-June 2021)

Daniel R. Obenour, PhD
Associate Professor, NC State University

20 July 2021

Contents

1. Overview

The first project year has provided several opportunities for engagement with the Falls Lake modeling team, which is led by the Upper Neuse River Basin Association (UNRBA). A list of our major activities includes:

1. In October 2020, we provided a memorandum on the segmentation of the WARMF-Lake model. This memorandum provided a theoretical basis for making segmentation decisions. The recommendations included splitting an existing segment at the Cheek Road causeway, which was adopted. See Appendix A for this memorandum.
2. In January 2021, we provided a memorandum for reconciling flows (in and out of Falls Lake) and thus closing the flow balance. We provided recommendations on how and where to make flow adjustments and what level of smoothing is appropriate for these adjustments. We also provided an illustrative example of how the smoothing algorithm works. Falls Lake modelers have been working to implement these recommendations. See Appendix B for this memorandum.
3. In May 2021, we had multiple meetings with UNRBA staff/modelers to address WARMF-watershed model calibration issues. A primary goal was to ensure that the model reasonably captured the sources and seasonality of nitrogen loading (nitrate, organic nitrogen, etc.). Suggestions were made for calibrating nitrogen transformation rates (e.g., nitrification, denitrification) and their associated temperature adjustment factors. Suggestions were also made regarding the representation of atmospheric nitrogen deposition. To help support this effort, we provided a review of available atmospheric nitrogen deposition data. This review is included here in Section 2.
4. In June 2021, we developed a geostatistical algorithm for assessing the probability of compliance with the state's water quality criteria, subject to different spatial monitoring resolutions and different mean levels of chl-a. This analysis was conducted in response to questions posed by UNRBA regarding how different monitoring strategies will influence compliance with water quality standards. See Section 3 for a discussion of preliminary results, which are being reviewed by UNRBA staff.
5. Because one of the major sources of uncertainty in developing future water quality scenarios, is the internal loading from reservoir sediment, we conducted a literature review of sediment phosphorus release rates across U.S. lakes and waterbodies. See Section 4 for our findings. We believe this review will provide important information for lake model calibration in the following year.
6. Finally, we regularly attended MRSW meetings (and some PFC meetings) to provide input on technical issues that arose during those meetings.

2. Review of atmospheric nitrogen deposition data

Kimia Karimi, Daniel Obenour

June 2021

Introduction

Total nitrogen deposition includes wet and dry nitrogen (N), both made up of oxidized and reduced portions. Wet deposition is the result of precipitation events (rain and snow) that removes particles and gases from the atmosphere. Dry deposition is the transfer of gases and particles to the landscape when there is no precipitation (Baumgardner et al., 2002). Oxidized N is primarily produced from the burning of fossil fuels, whereas reduced N is primarily emitted from agricultural and livestock systems. Reduced N includes both Ammonia (NH_3) and particulate Ammonium (NH_4^+). Oxidized N mainly comprises nitrogen oxide (NO), nitrogen dioxide (NO_2), and nitric acid (HNO_3) (Paerl et al., 2002). However, more comprehensive definitions of oxidized N include HNO_3, NO_x, Dinitogen pentoxide (N_2O_5), Nitrous acid (HONO), organic nitrates, and Peroxyacyl nitrates (PAN) (Schwede and Lear, 2014).

N deposition Databases

Total Deposition Science Committee (TDEP)

EPA has developed a hybrid approach to mapping total deposition that combines measured and modeled values (Schwede and Lear, 2014). This Total Deposition Science Committee (TDEP) was formed within the National Atmospheric Deposition Program (NADP) in 2011. Wet deposition values are obtained from combining NADP/National Trends Network (NADP/NTN) measured values of precipitation chemistry with precipitation estimates from the Parameter-elevation Regression on Independent Slopes Model (PRISM). Dry deposition values are obtained by combining air concentration data with modeled deposition velocities. Air concentration data are from the Clean AirStatus and Trends Network (CASTNET), the NADP/Ammonia Monitoring Network (NADP/AMoN), and the Southeastern Aerosol Research and Characterization (SEARCH) network, while deposition velocities are estimated from the Community Multiscale Air Quality (CMAQ) model. These point values for deposition are merged spatially with modeled dry deposition values from the CMAQ model. CMAQ predicts hourly concentration and deposition values using a numerical air quality model (Byun and Schere, 2006).

TDEP maps are available for dry, wet, and total deposition. Dry N deposition is available for total N, reduced N, oxidized N, total Nitrate, and Ammonium, while wet N deposition is available for inorganic N, Nitrate (NO_3^-), and Ammonium. Finally, total deposition in availablefor total N, reduced N, and oxidized N. The total Nitrate (in the dry deposition) refers to HNO_3 and particulate NO_3 (TDEP). Based on an NADP brochure, inorganic N deposition contains Ammonium and Nitrate depositions. However, comparing maps of inorganic N, Ammonium, and Nitrate wet depositions shows that wet Nitrate depositions are higher than the other two (perhaps due to a nitrate mapping error). TDEP maps can be found in https://www3.epa.gov/castnet/mapcharts.html, but the underlying data are not available for online download. A semi-quantiative exploration of these maps shows that in our study area, total N deposition is likely dominated by oxidized N, especially in urban areas (Figure 1). Total deposition of oxidized N in urbanized areas is approximately 2 times higher than rural areas, whereas reduced N is higher in the livestock regions east of our study area (Figure 1). The dry N deposition is also dominated by the oxidized portion, particularly in urban areas (Figure 2). Dry N deposition has decreased from 2000 to 2019 (Figure 3) mainly due to the decrease in the oxidized portion. The dry N deposition does not

appear to be correlated with precipitation. The wet inorganic N deposition has decreased gradually from 2000 (dry year) to 2019 (wet year) (Figure 4). This is true even though (comparing more maps from 2000-2019) wet inorganic N deposition is generally higher in wet years.

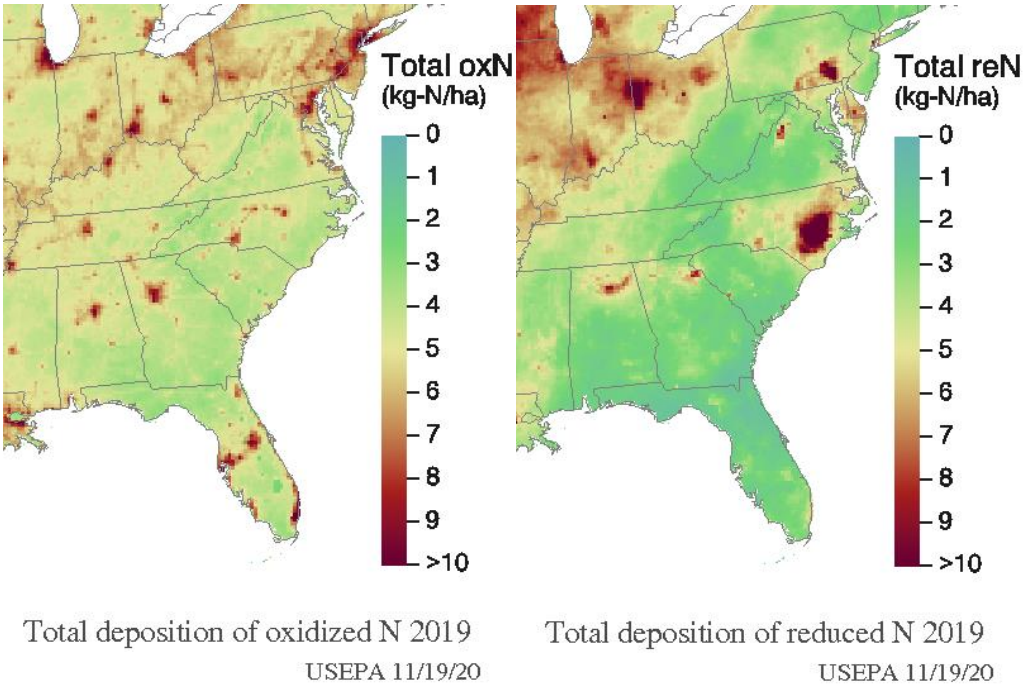

Figure 1. Total deposition of oxidized (left) and reduced (right) N in 2019 (https://www3.epa.gov/castnet/mapcharts.html).

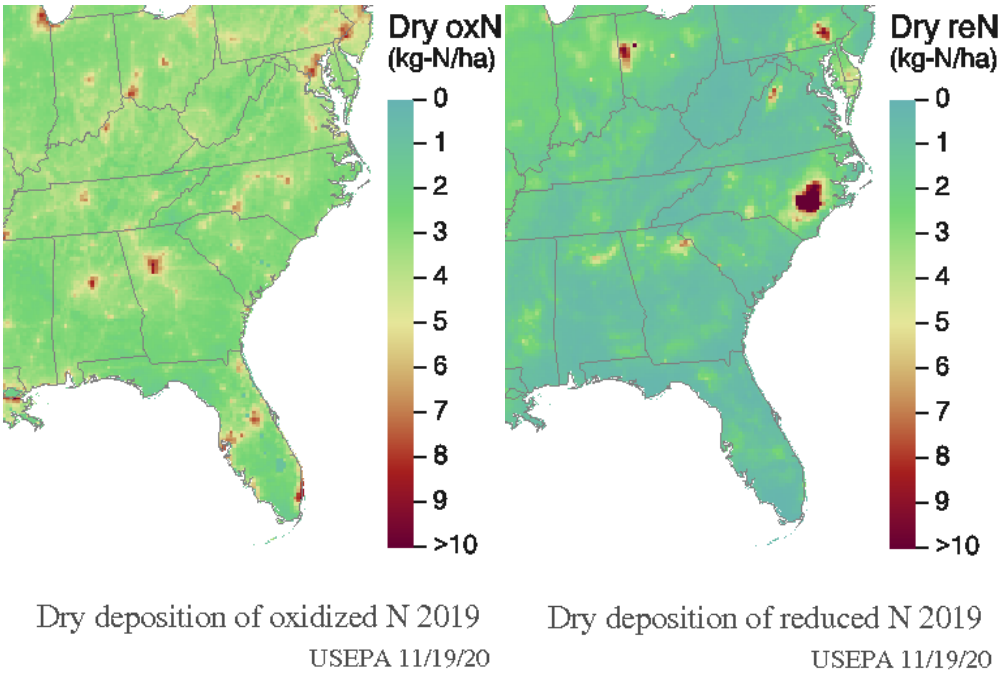

Figure 2. Dry deposition of oxidized (left) and reduced (right) N in 2019 (https://www3.epa.gov/castnet/mapcharts.html).

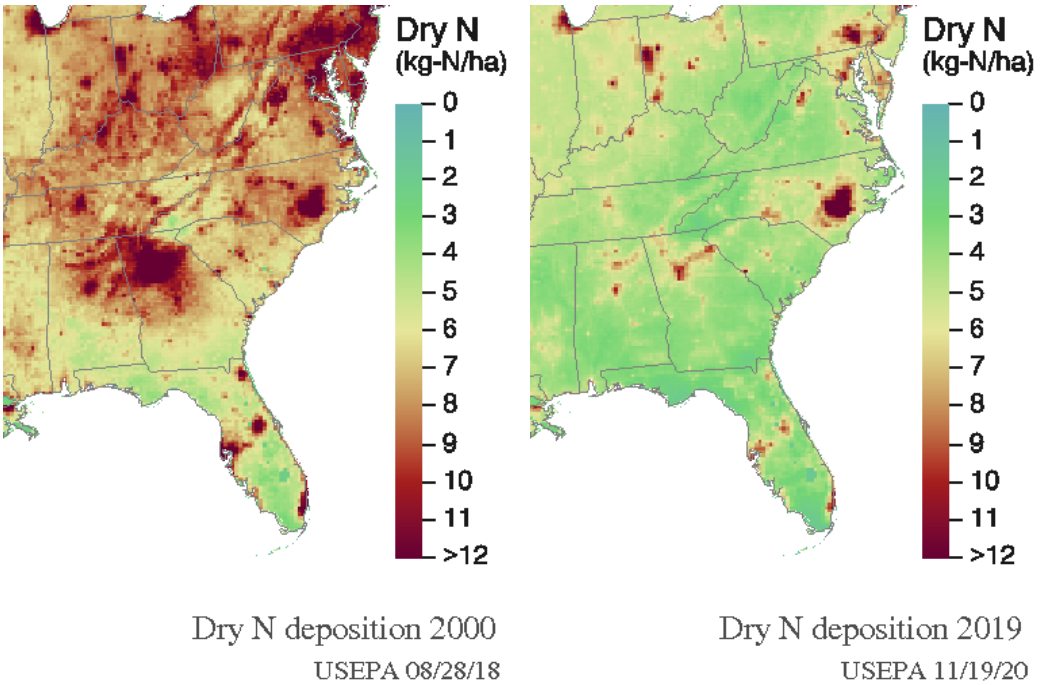

Figure 3. Dry N deposition in 2000 (left) and 2019 (right) (https://www3.epa.gov/castnet/mapcharts.html).

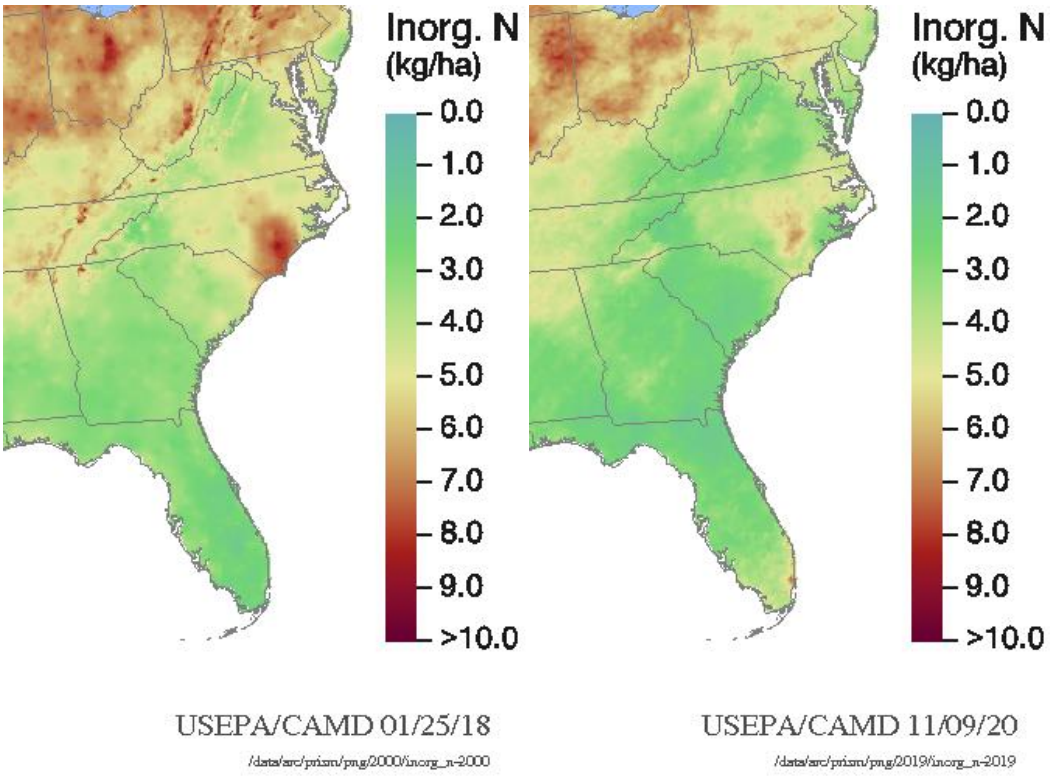

Figure 4. Wet deposition of inorganic N in 2000 (left) and 2019 (right) (https://www3.epa.gov/castnet/mapcharts.html).

The NADP National Trends Network (NTN)

The NADP NTN (http://nadp.slh.wisc.edu/ntn/) has a long-term record of precipitation chemistry and wet deposition at over 250 stations in the U.S. It collects weekly precipitation samples and measures a number of analytes including SO_4, NO_3, and NH_4 (Schwede and Lear, 2014).The NTN sites located in the Piedmont region are (Figure 5, Table 1). NTN provides weekly concentrations, seasonal and annual wet depositions (Figure 6).

Figure 5. Location of the NTN/NADP stations.

Table 1. NTN station description.

Site ID	Location	Nearest city	Data availability
NC 30	Duke Forest	Durham	2020
NC 17	Greensboro	Greensboro	2015-2019
NC 11	Research Triangle Institute	Durham	1980-1982
NC 33	Research Triangle Park	Durham	1980-1983
NC 34	Piedmont Research station	Salisbury	1978-2019
NC 41	Finley Farm	Raleigh	1978-2019

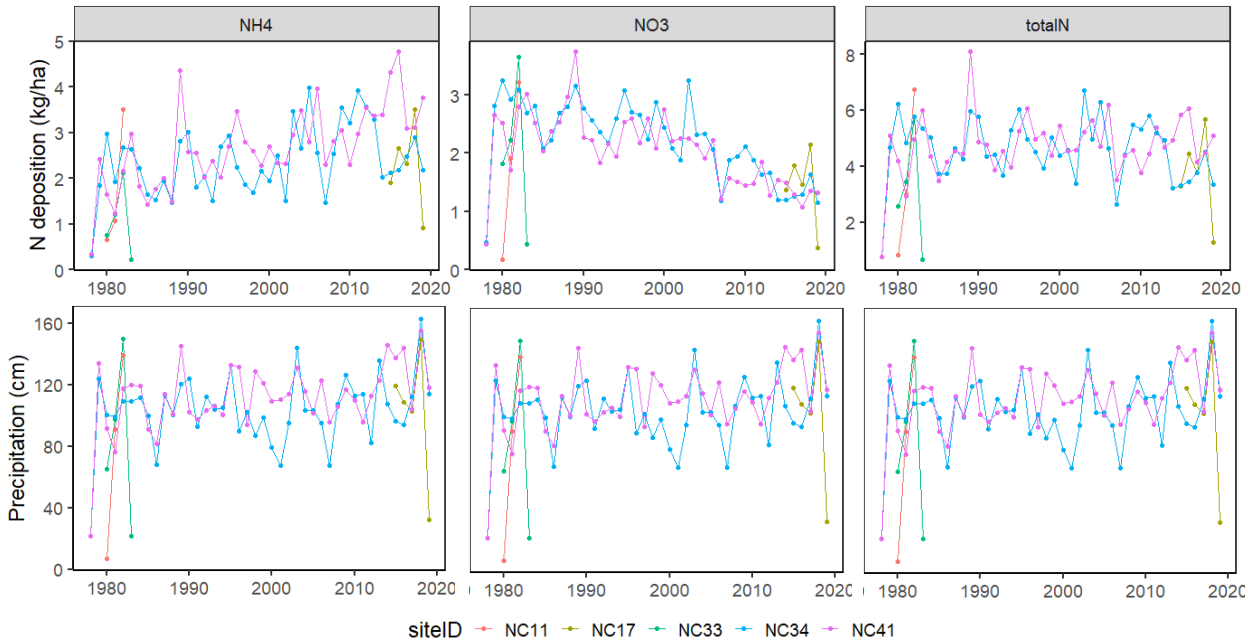

Figure 6. NTN annual wet N deposition (upper) and precipitation (lower).

The median NTN (wet) deposition for NH_4, NO_3, and total N for these stations are 2.4, 2.2, and 4.6 kg/ha/y, respectively. The higher deposition values mostly correspond with higher precipitation years. However, the correlation between annual deposition and precipitation varies in each form of N, with the lowest correlation with NO_3 (Table 2). On average, the total N wet deposition in wet years is about 5.5 kg/ha/y, while in dry years it is about 3.8 kg/ha/y. The total N and NH_4 wet deposition values are generally consistent with the TDEP inorganic N and NH_4 wet deposition; however, NO_3 wet deposition values from NTN measurements are lower than the TDEP values.

Table 2. Correlation of precipitation with each N form of annual deposition from NTN measurements. The values are shown for the two stations that had the longest record.

NTN site\variable	NH_4	NO_3	Total
NC34	0.59	0.35	0.61
NC41	0.73	0.30	0.77

The monitored values can also be summarized by season to explore the seasonal variability of N deposition (Figure 7). The boxplot of each N form deposition shows higher deposition in spring and summer, which is likely related to higher precipitation in these seasons, especially in late summer. These results also indicate substantial year-to-year variability in seasonal wet N deposition.

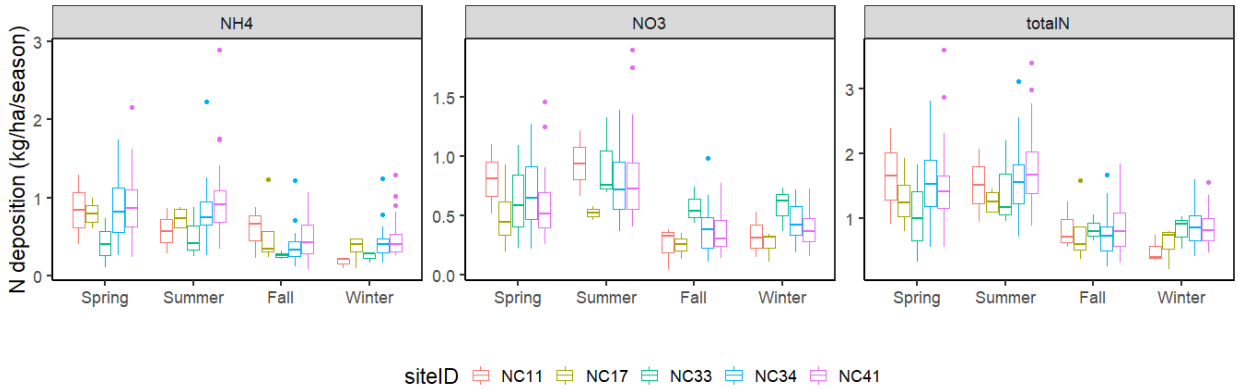

Figure 7. Seasonal wet N deposition from NTN measurements.

Clean AirStatus and Trends Network (CASTNET)

CASTNET (www.epa.gov/castnet) measures ambient concentrations of sulfur and nitrogen species as well as rural O_3 concentrations. The concentrations are used to calculate dry deposition fluxes. It complements NTN, with nearly all sites co-located with or near an NTN site. The CASTNET monitoring network has 2 stations in the Piedmont region located in Duke Forest and Research Triangle Park. These two sites are close to NC30 and NC33, however, they provide a longer and more recent record than NTN measurements (from 2000-2017). The CASTNET website provides dry, wet, and total N annual deposition (Figure 8). Similar to TDEP maps (Figures 3), Figure 8 shows that dry N deposition has decreased over time. Wet N deposition has more variability due to its positive correlation with precipitation (Table 3). The median total, wet, and dry deposition values are 12.2, 4.9, and 7.3 kg/ha, respectively. The median wet deposition from CASTNET measurements (4.9 kg/ha) is close to the NTN measurement (4.6 kg/ha). On average, dry deposition makes up 60% of total N deposition in these two stations. This is generally consistent with the information from the TDEP maps.

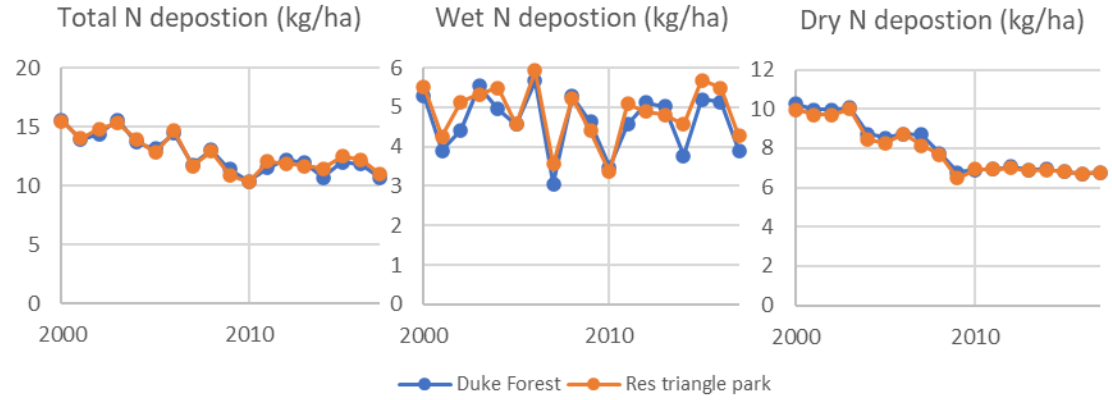

Figure 8. Total, wet, and dry N deposition from CASTNET.

Table 3. Correlation of precipitation with annual wet and dry N deposition from CASTNET measurements.

CASTNET site\variable	Wet N deposition	Dry N deposition
Duke Forest	0.71	-0.21
Research Triangle Park	0.62	-0.04

Baumgardner et al. (2002) collected data as part of the CASTNET deposition monitoring conducted during the 1990s. Dry deposition contributed approximately 35% of total nitrogen deposition in North Carolina, rather than the 60% observed in the more recent CASTNET data for our study area (above). This discrepancy may be due to using older measurements (1990s) as well as using different monitoring sites.

Community Multiscale Air Quality (CMAQ) model

CMAQ is an advanced regional air quality model developed by EPA to simulate the fate, transport, and deposition of air pollutants under varying atmospheric conditions (Byun and Schere, 2006). The data provides hourly estimates and aggregated daily datasets from 2002-2014 (https://www.epa.gov/cmaq/cmaq-output). The output shapefile is also available through their FTP server. There are some databases that computed aggregated annual CMAQ estimates.

EnviroAtlas national map is an interactive map that portrays annual nitrogen deposition (kg/ha/y) within each 12-digit hydrological unit code (HUC) watershed for 2011 (which is a fairly normal precipitation year for the study area). This map provides information from the CMAQ model (https://enviroatlas.epa.gov/enviroatlas/interactivemap/). The map provides annual wet, dry, and total deposition for reduced and oxidized N deposition (Figures 9-12). Comparing the CASTNET values in 2011 with this interactive map shows that the values are similar (less than 10% difference).

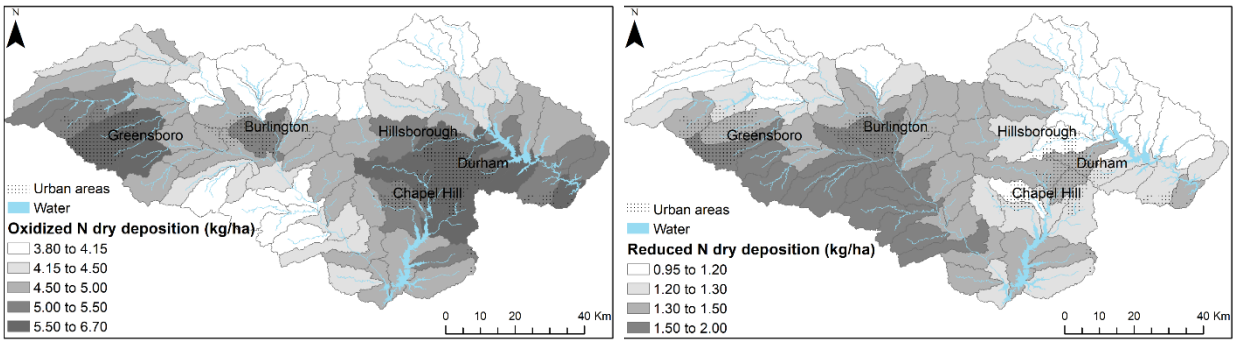

Figure 9. Dry annual oxidized (left) and reduced (right) N deposition (from EnviroAtlas national map).

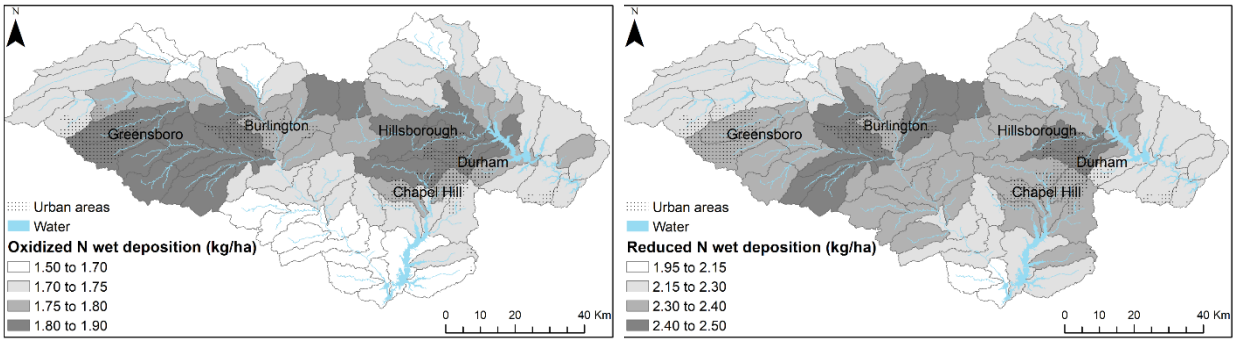

Figure 10. Wet annual oxidized (left) and reduced (right) N deposition (from EnviroAtlas national map).

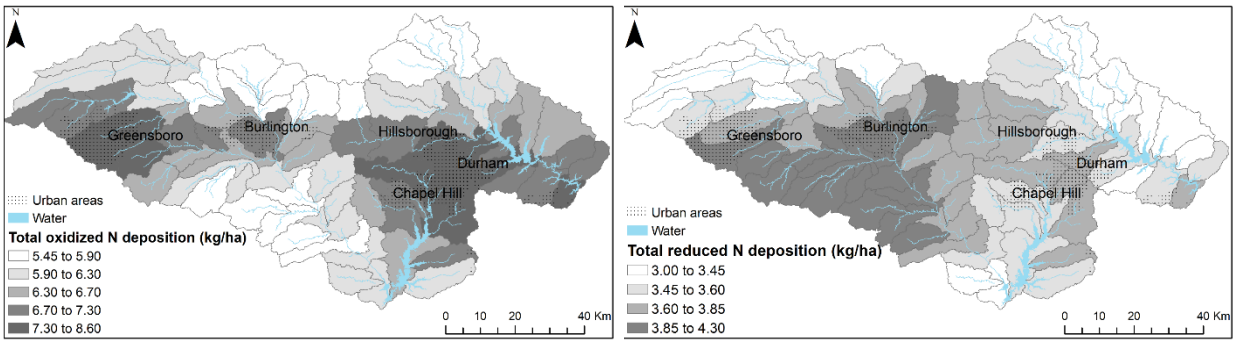

Figure 11. Total annual oxidized (left) and reduced (right) N deposition (from EnviroAtlas national map).

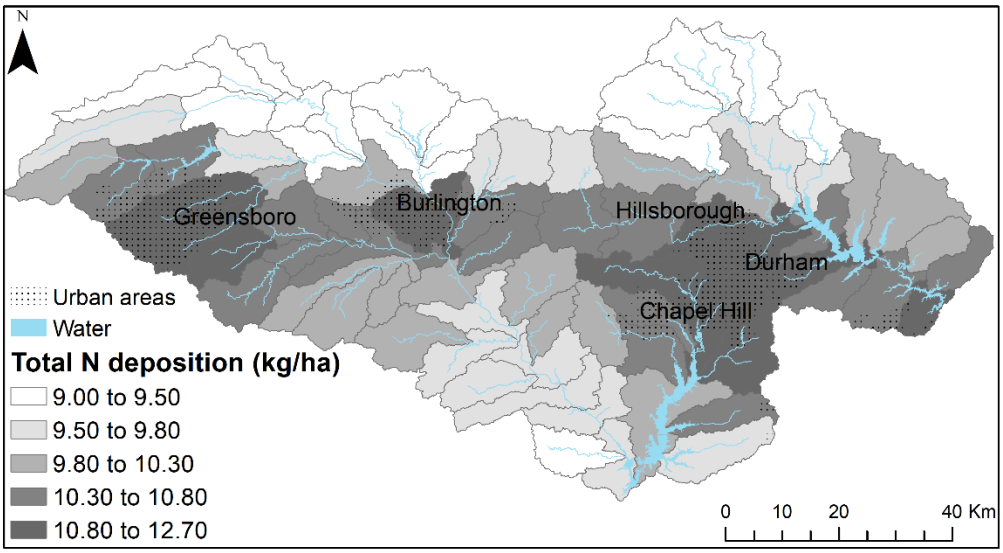

Figure 12. Total N deposition (from EnviroAtlas national map).

The oxidized N deposition values are higher in urban areas, especially in Greensboro and Durham (Figures 9-11, left). However, the reduced wet and dry N deposition does not show a strong spatial pattern related to urbanization (Figures 9-11, right). The median N deposition for each form is provided in Table 4. N dry deposition and total N deposition are both dominated by the oxidized form. This complies with the findings of the TDEP maps (Figures 1-2). Unlike dry and total N deposition, wet deposition is dominated by the reduced form. The wet Ammonium deposition maps from TDEP also shows its dominance in the inorganic N deposition. However, since TDEP does not provide wet Ammonia deposition maps, comparing wet deposition from the EnviroAtlas map and TDEP maps is not straightforward. Finally, dry deposition (median= 5.89 kg/ha) is the dominant form of total deposition. The dry deposition makes up about 60% of total deposition, which complies with the CASTNET measurements.

Table 4. Median deposition values (kg/ha/y) for each N form in Figures 9-12.

Deposition type	Oxidized	Reduced	Total
Wet	1.74	2.32	4.06
Dry	4.61	1.29	5.89
Total	6.41	3.59	10.05

The USGS SPARROW model for North Carolina includes N deposition as an input variable (Gurley et al., 2019). The model input is a 3-year average (2010, 2011, 2012) of total deposition (Figure 13) derived from a national database (Wieczorek et al., 2018). Wieczorek et al. (2018) created national databases of information (including annual N deposition from the CMAQ model) linked to the National Hydrography Dataset-Plus (NHD+) catchments (Moore and Dewald, 2016). These estimates are aggregated based on NHD+ catchments (not shown in Figure 13). Instead, Figure 13 shows the HUC12 boundaries for visualization purposes. The deposition maps show higher N deposition in urbanized areas. The median total N depositions in 2010, 2011, and 2012 are 9.65, 10.22, and 10.52 kg/ha, respectively. Comparing Figure 13 with the EnviroAtlas map (Figure 12) shows that the total deposition values are close.

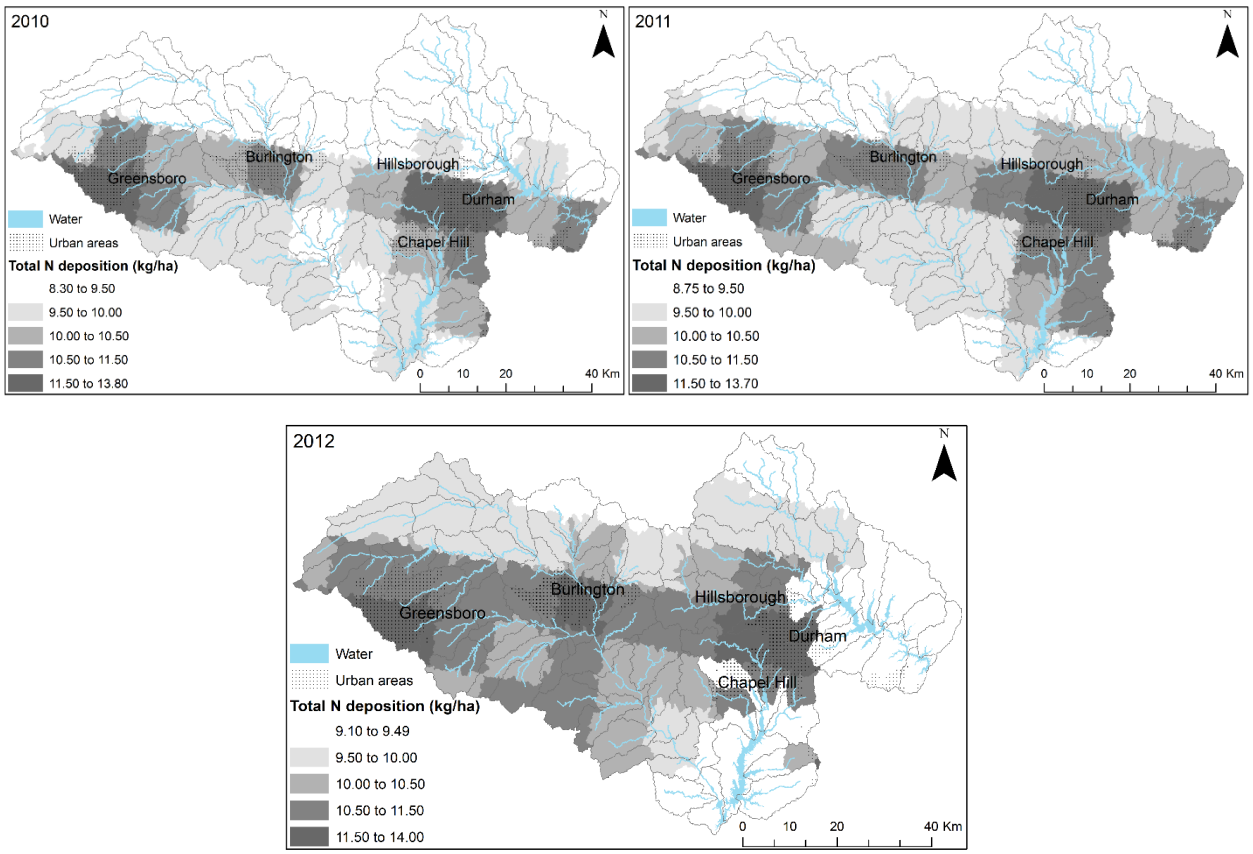

Figure 13. Total (wet + dry) N deposition in 2010 (left), 2011 (right), and 2012 (lower) from (Wieczorek et al., 2018).

Summary

- The median total annual N deposition for the study area is 12 kg/ha/y based on CASTNET data (2000-2017).
- Spatially distributed estimates of total N deposition for 2010-2012 range from 8-14 kg/ha/y (Wieczorek et al., 2018).
- Total N deposition is highest in summer, followed by spring, mainly due to higher precipitation in our study area during these seasons (NTN).
- Total annual N deposition is positively correlated with annual precipitation. This is primarily due to precipitation increasing wet deposition (NTN and CASTNET).

- Dry N deposition makes up about 60% of total deposition (EnviroAtlas map and CASTNET).
- Total N deposition is higher in urban areas, primarily due to higher dry oxidized deposition (TDEP and EnviroAtlas map).
- Oxidized N accounts for 40% of wet deposition, 80% of dry deposition, and 65% of total deposition (EnviroAtlas map).

References

Baumgardner, R. E., Lavery, T. F., Rogers, C. M. and Isil, S. S. (2002) 'Estimates of the atmospheric deposition of sulfur and nitrogen species: Clean Air Status and Trends Network, 1990-2000', *Environmental Science and Technology*, 36(12), pp. 2614–2629. doi: 10.1021/es011146g.

Byun, D. and Schere, K. L. (2006) 'Review of the governing equations, computational algorithms, and other components of the models-3 Community Multiscale Air Quality (CMAQ) modeling system', *Applied Mechanics Reviews*. American Society of Mechanical Engineers Digital Collection, pp. 51–76. doi: 10.1115/1.2128636.

Gurley, L. N., Garcia, A. M., Terziotti, S. and Hoos, A. . (2019) 'SPARROW model datasets for total nitrogen and total phosphorus in North Carolina, including simulated stream loads', *Journal of Chemical Information and Modeling*, 53(9), pp. 1689–1699. doi: 10.1017/CBO9781107415324.004.

Moore, R. B. and Dewald, T. G. (2016) 'The Road to NHDPlus - Advancements in Digital Stream Networks and Associated Catchments', *JAWRA Journal of the American Water Resources Association*. Blackwell Publishing Inc., 52(4), pp. 890–900. doi: 10.1111/1752-1688.12389.

Paerl, H. W., Dennis, R. L. and Whitall, D. R. (2002) 'Atmospheric deposition of nitrogen: Implications for nutrient over-enrichment of coastal waters', *Estuaries*, 25(4), pp. 677–693. doi: 10.1007/BF02804899.

Schwede, D. B. and Lear, G. G. (2014) 'A novel hybrid approach for estimating total deposition in the United States', *Atmospheric Environment*, 92, pp. 207–220. doi: 10.1016/j.atmosenv.2014.04.008.

Wieczorek, M. E., Jackson, S. E. and Schwarz, G. E. (2018) *Select Attributes for NHDPlus Version 2.1 Reach Catchments and Modified Network Routed Upstream Watersheds for the Conterminous United States - ScienceBase-Catalog*. doi: https://doi.org/10.5066/F7765D7V.

3. Chlorophyll a simulator for compliance assessment

Daniel Obenour

June 2021

In meetings with UNRBA modeling and regulatory support staff, questions arose regarding the relationship between spatial resolution (monitoring and modeling) and compliance with NC water quality criteria (standards). To explore these issues, a geostatistical model was developed to create statistical simulations of chl-a at various monitoring resolutions considering the historical chl-a observations (2014-2018) and the spatial correlation structure of those observations. An example application of this geostatistical simulator is provided below. In the future, it is anticipated that the simulator will be applied to other monitoring scenarios and chl-a assessment criteria. Code is available to others upon request.

The geostatistical model was developed using conventional methods (Chiles & Delfiner, 2009). Chl-a data were power-transformed so that they could be accurately modeled as a Gaussian process (Fig 2.1). Distances between stations were measured along the main stem of the reservoir, and lateral offsets were determined for stations on the reservoir arms. Spatial covariance was estimated using an exponential variogram function fit to an experimental (data-derived) variogram through least squares optimization. The variogram indicates that observations are correlated within about 15 km (Fig 2.2). Geostatistical conditional simulations (5000) were run to generate spatially-consistent Monte Carlo samples of chl-a for each month (2014-2017) at up to 11 hypothetical monitoring stations along the main stem of Falls Lake.

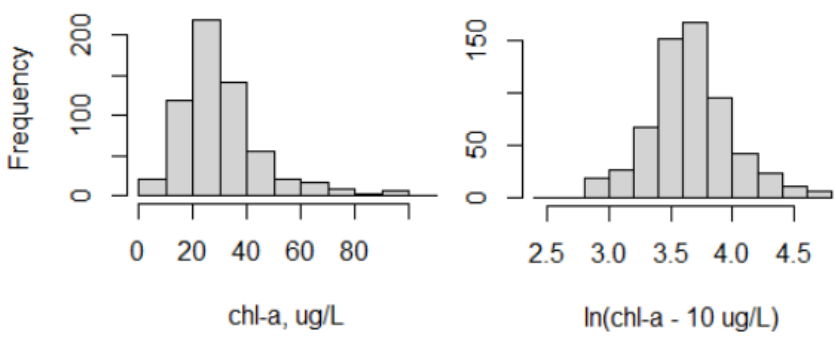

Figure 2.1: Original (left) and power-transformed (right) chl-a datasets used in the geostatistical simulation.

For an example application, we evaluate the probability of lake compliance using a simple chl-a criterion. Specifically, the lake is considered in compliance when no more than 1 out of 12 monthly samples exceed 40 ug/L at any monitoring site in a randomly selected year. Results (Figure 2.3) are shown for different numbers of monitoring sites along the main stem of Falls Lake (3 to 11 sites) and different multipliers of historical chlorophyll levels (0.4 to 1.2). The probability of a violation (i.e., non-compliance) considers spatial stochasticity as well as interannual variability. Note that all of these simulations include at least one location near the upstream end of the lake (near station NEU013B), where chl-a levels are typically highest. For this particular case, we see that increasing the number of monitoring sites will modestly increase the probability of violation for multipliers of 0.6 and 0.8. For lower and higher multipliers, there is a strong tendency for compliance and violation, respectively, regardless of the number of monitoring sites.

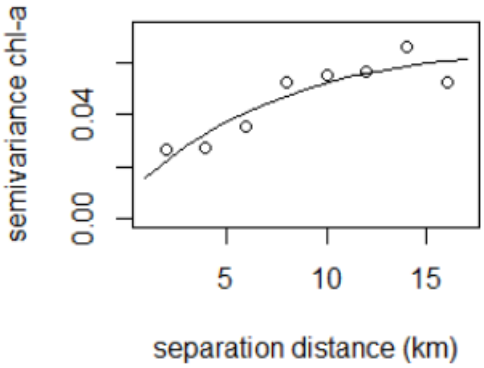

Figure 2.2: Experimental variogram (circles) and fitted exponential variogram/covariance function (line).

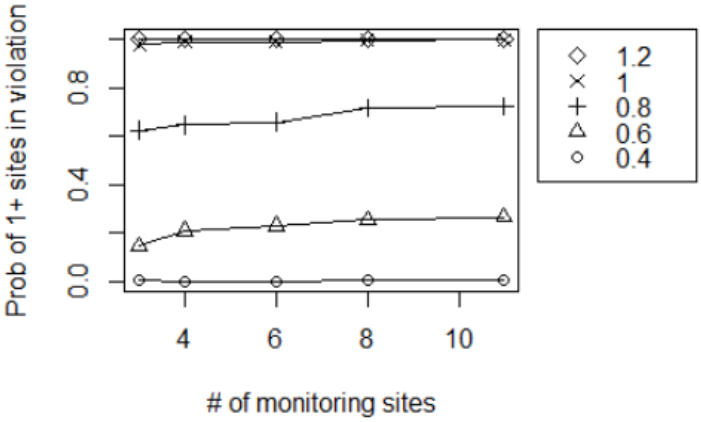

Figure 2.3: Probability of one or more monitoring sites in violation of chl-a criteria versus number of monitoring sites. Results are shown for various multipliers of existing chl-a concentrations (shown in legend).

References:

Chiles, J. P., & Delfiner, P. (2009). Geostatistics: modeling spatial uncertainty (Vol. 497). John Wiley & Sons.

4. Review of sediment phosphorus release for U.S. lakes and reservoirs

Smitom Borah, Daniel Obenour July 2021

Introduction

One of the biggest challenges to the management and protection of water bodies across the world is eutrophication (Le Moal et al., 2019). This has led to the development of management strategies that aim to reduce nutrient inputs and thereby minimize the source for eutrophication. One potentially important input is the recycling of nutrients from the lake (or reservoir) bottom sediments. Such recycling can delay benefits from external mitigation efforts (James et al., 1995). This source is often referred to as internal loading, though it may reflect the accumulation of external loads over long time periods. As phosphorus (P) is often the limiting nutrient in freshwater systems (Schindler et al.,2016), in this memorandum, internal P loading from the sediment layer in different shallow US lakes and reservoirs is discussed.

Release of P from the sediments is a complex dynamic process, driven by competing biogeochemical mechanisms. One of the prominent mechanisms is the reductive desorption of P from ferric ions under anaerobic conditions with subsequent upward diffusion from the sediment layer (Mortimer, 1942). Given its effectiveness and simplicity, this model, sometimes referred to as the 'classical model', is often cited to explain internal P loading under anoxic conditions. However, the classical model may not always be the driving mechanism for sediment P release (Sondergaard et al., 2001). Decomposition of organic matter in eutrophic and hypereutrophic lakes, irrespective of the extent of oxic condition, can also mobilize a substantial fraction of organic P into internal P loading (Hupfer and Lewandowski, 2008). Vertical mixing due to wind action, as well as bioturbation, can also contribute to P release from the sediments (Reddy et al., 1996; Sondergaard et al., 2001; Orihel et al., 2017). Many studies have also cited excretion of exudates from benthic biota as a probable mechanism for sediment P release (Orihel et al., 2017).

The dominance of these mechanisms in a particular water body largely depends on the dynamics of many factors such as pH, temperature, water hardness and concentration of iron, aluminum, nitrate, and sulphate in that body. In soft-water systems with significant iron and aluminum content in the sediments, sediment P releases tend to increase with increase in pH on account of higher competition between hydroxide and phosphate ions for ligand exchange (Olila and Reddy, 1995). On the other hand, in hard-water systems, sediment P releases tend to decrease with increasing pH due to co-precipitation of P with calcium ions. Temperature also plays a crucial role in sediment P release mechanisms. With increases in temperature, microbial reduction of iron bound P as well as decomposition rates are enhanced and thereby release rates of sediment P is further accelerated (Orihel et al., 2017). The extent of sediment aluminum concentration is another key factor in sediment P release. Aluminum bound P tends to have lesser susceptibility to redox related dissociation (Hupfer and Lewandowski, 2008). The presence of nitrates and sulphates near the sediment-water interface (SWI) adds another layer of complexity to the classical model (Hemond and Lin, 2010). Nitrates can act as electron acceptors, a role usually played by dissolved oxygen in the classical model, to oxidize ferrous ions and thereby reduce the

sediment P release rate under anaerobic conditions. Sulphates, on the other hand, play the contrary role. Within the sediment layer, sulphates remove ferrous ions, which reduces the potential for Fe-P mineralization. Sulphates also compete with phosphate ions for sorption sites (Orihel et al., 2017).

The objective of this memorandum is to summarize and compare sediment P release fluxes determined for various shallow lakes across the US using different estimation methods. The most common method was sediment core incubation, in which intact sediment cores were incubated in a controlled laboratory environment and P concentration in the overlying water was measured at various frequencies. These studies measured soluble reactive phosphorus (SRP, sometimes also referred to as dissolved reactive phosphorus or DRP), total dissolved phosphorus (TDP) or total phosphorus (TP), but it is generally expected that most of the released phosphorus will be in the form of SRP. The sediment release flux was then calculated based on the rate of P accumulation in the overlying water column. Another method was the application of box chambers. Here, the calculation of P flux was essentially the same, but this method was applied *in-situ*. In some other studies, the sediment P release flux was measured by calculating the diffusive flux of P from the sediment layer using Fick's Law (typically from sediment cores). In addition, some researchers estimated sediment P release based on the changes in hypolimnetic P over short time periods. Long-term datasets can also be used to estimate sediment P release rates, particularly when combined with mass-balance modeling (Chapra and Canale, 1991; Jensen et al., 2006).

Sediment P release flux in different shallow lakes

The average estimate of sediment P release flux of different shallow US lakes and reservoirs under aerobic and anaerobic conditions are reported in Table 1. These lakes and reservoirs are classified as shallow based on either common perception or location in generally flat topography, with smaller surface area (0.4 to 39 km^2). Additionally, all water bodies were classified as either eutrophic or hypereutrophic in their respective studies. Except the study on the Western Basin of Lake Erie, sediment core incubation was carried out to determine sediment P release flux. The average sediment P release fluxes reported in Lake Erie is the mean value of different sediment P release fluxes measured by various techniques under aerobic and anaerobic conditions. In lakes, Lake Mendota, Lake Wingra and Little John Lake, the reported P release flux is an average of different values observed under varying conditions of incubation temperature and stirring rate. All values of P reported in Table 1, except that for Long Lake, are based on the experimentally measured SRP values. The average sediment P release flux in Long Lake is based on TDP measurement.

Results from sediment core incubation studies indicate that both aerobic and anaerobic P release fluxes vary greatly across different studies (Table 1). Typically, P release fluxes are higher under anaerobic conditions. This suggests a strong relationship with the redox environment near the SWI (classical model). In fact, this is clearly evident in lakes such as Lake Eucha, Lake Okeechobee and Lake Erie, where the anaerobic P release fluxes were higher than those under aerobic condition by about 330%, 450% and 350%, respectively. Interestingly, the variation in the observations in Table 1 also suggest the prevalence of other factors that affect the sediment P release flux.

Table 1. Sediment P release flux from sediment core incubation studies

Lake or reservoir	State	Period of Observation (Year)	Mean depth (m)	Incubation temperature	Average sediment P release flux ($g/m^2/month$)		References
					Aerobic condition	Anaerobic condition	
Lake Apopka[c]	FL	Annual (Pre 1990)	2	25	0.08	-	Moore Jr. et al. (1991), Havens et al. (1999)
Lake Eucha (reservoir)	OK	April (2002)	-	22	0.03	0.13	Haggard et al. (2005)
Lake Halfmoon	WI	June – July (2010 – 2015)	1.6	20	-	0.31	James (2017)
Lake Pepin	MN	June – August (1992)	5	25	0.11	0.46	James et al. (1995)
Wind Lake	WI	October (1995 – 1996)	2.9	20	0.15	0.25	James et al. (2000)
Western Basin, Lake Erie[a]	-	June – July (2013 – 2014)	7.3	20	0.04	0.18	Matisoff et al. (2016)
Lake Okeechobee	FL	June (1989), September (1989), January (1990), March (1990)	2.7	22	0.02	0.12	Moore et al. (1998)
Long Lake[b]	WA	April (1978), August (1978)	2	-	0.07	-	Jacoby et al. (1982)
Lake Mendota	WI	April (1973), July – October (1973), January (1974), March (1974), July – August (1974)	12.8	-	0.40 (0.06[e])	1.1[d] (1.1[e])	Holdren and Armstrong (1980)
Lake Wingra	WI	February – April (1974), June (1974)	2.7	-	0.02	0.05[d]	
Little John Lake	WI	March (1973), June (1975)	-	-	0.02	0.06[d]	
Banner Creek reservoir	KS	June – August (2010)	-	17	-	0.14	Carter and Dzialowski (2012)
Big Creek reservoir	IA		-		-	0.49	
Bluestem reservoir[c]	NE		-		-	0.73	
Cheney reservoir[c]	KS		-		-	1.23	
Conestoga reservoir[c]	NE		-		-	0.41	
Easter reservoir	IA		-		-	0.09	
El Dorado reservoir	KS		-		-	0.03	
Gardner reservoir	KS		-		-	0.39	
Marion reservoir[c]	KS		-		-	1.00	
Olathe reservoir	KS		-		-	0.29	
Pomona reservoir	KS		-		-	0.33	

Winfield reservoir	KS		-		-	0.86	
Wagontrain reservoir[c]	NE		-		-	0.53	

[a] Average of internal P release rate based on different sampling methods is reported here
[b] Average sediment P release rate is based on apparent loss of TDP from sediment cores
[c] Hypereutrophic
[d] Complete anaerobic condition was not observed in the study
[e] Median value

In Wind Lake, the P release flux under aerobic conditions (0.15 g/m^2/d) was several times higher than most other lakes. One possible reason for such high release could be the presence of relatively high levels of organic P in the sediments (James et al., 2000), resulting in P release due to microbial decomposition. Consequently, in comparison to Lake Eucha, Lake Okeechobee and Lake Erie, there was only a 69% increase in sediment P release when the sediment cores were incubated under anaerobic conditions. In fact, relatively high aerobic P release fluxes for Lake Apopka and Long Lake can also be partly attributed to the microbial decomposition of organic matter (Jacoby et al., 1982; Moore Jr. et al., 1991).

Lake Pepin provides another interesting insight into sediment P release flux. In the study carried out by James et al. (1995), the researchers observed that NaOH-P was the dominant fraction in the sediment layers. This fraction accounts for iron- and aluminum-bound P along with some amount of organic P (Moore et al. 1998). The same study also pointed out that pH in Lake Pepin was usually greater than 8.0. This might cause higher P release under aerobic conditions, as NaOH-P retention in sediments is reduced at higher pH levels. Interestingly, if sediments in Lake Pepin had the largest fraction of HCl-P, which accounts for calcium bound P, the role of pH in P retention would be reversed. This could be another possible explanation for such low aerobic P release in Lake Okeechobee that has high calcium ions concentration (Pollman and James, 2011).

In some of the lakes, such as Lake Apopka and Lake Pepin, higher aerobic P release fluxes could be also attributed to relatively higher incubation temperature than other studies in Table 1. For example, a continuation of the study carried out by Matisoff et al. (2016) in Western Basin of Lake Erie showed that the average sediment P release flux under anaerobic conditions increased from 0.08 g/m^2/month to 1.12 g/m^2/month when incubation temperature was raised from 10°C to 30°C (Gibbons and Bridgeman, 2020). This implies a very large temperature adjustment factor (θ) of 1.14 for P fluxes (Chapra, 2008). Similarly, elevated fluxes were also observed in Lake Mendota, Lake Wingra, and Little John Lake when incubation temperature was raised with other factors kept constant.

The study carried out by Gibbons and Bridgeman (2020) also highlighted the role of sediment P concentration in release flux. After 4 days of anaerobic incubation at 30°C, the sediment core with nearly 1 mg P/g yielded about 80 g/m^2/day (2.43 g/m^2/month) of average sediment P release flux whereas the sediment core with about 0.55 mg P/g yielded 4.27 g/m^2/day (0.13 g/m^2/month) of average sediment P release flux. Thus, varying sediment P concentrations could be another explanation for variability in P release within and across lakes and reservoirs.

The results for Lake Mendota emphasize another important mechanism for sediment P release. While the average value for aerobic sediment P release flux was observed as high as 0.40 $g/m^2/month$, the corresponding median value was only 0.06 $g/m^2/month$. This stark difference in the central measures is likely due to bio-irrigation amplifying P release in some samples. In the study carried out by Holdren and Armstrong (1980), the authors pointed out that high sediment P release (independent of temperature, mixing, and oxic conditions) was observed in some of the sediment cores that had abundant tubificids and chironomid larvae. Interestingly, the sediment P release in those sediment cores had an average flux of nearly 2 $g/m^2/month$.

The sediment core incubation studies may underestimate the actual sediment P release flux, primarily due to algal and/or microbial P uptake and P sorption by the container material (Matisoff et al., 2016). Moreover, as these studies are carried out in a laboratory environment, it is unlikely that the complex natural ecosystem at the SWI can be replicated entirely. Many studies do not account for wind action, which can play an important role in P release in shallow water bodies. Table 2 shows some of the lakes and reservoirs in the US where *in-situ* measurements of average sediment P release have been attempted. Different approaches were adopted in different studies. Sediment P releases in Lakes Erie and Pepin are reported for SRP, whereas releases for Lake Shagawa and Tenkiller Reservoir are reported as TP.

Table 2. *In-situ* sediment P release flux.

Lake or reservoir	Period of Observation (Year)	Surrounding condition	Avg sed P release flux ($g/m^2/month$)	References
Central basin, Lake Erie	July – October (2019)	Anaerobic	0.78	Anderson et al. (2021)
Tenkiller Reservoir[a]	June – September (2005), May – September (2006)	Anaerobic	0.46	Cooke et al. (2011)
Lake Shagawa	June – August (1971 – 1975)	Anaerobic	0.31	Larsen et al. (1981)
Lake Pepin	July – August (1992)	Aerobic	0.15	James et al. (1995)

[a] Tenkiller Reservoir has a mean depth of 15 m and can be regarded as a deep reservoir

When compared with Table 1, the Table 2 sediment P release fluxes are generally higher in comparable lakes. In Lake Pepin, the *in-situ* sediment P release flux is just about 30% higher than that in the sediment core study, whereas the *in-situ* sediment P release flux in central Lake Erie is about 300% higher than the sediment core study for the Western Basin of this lake. This is particularly surprising, considering that the central basin of Lake Erie is deeper and less eutrophic. One probable reason for such higher results could be the unique (*in-situ*) monitoring method adopted for the study (Anderson et al., 2021).

Sediment P release in Jordan Lake

Jordan Lake is a shallow reservoir (mean depth = 4.70 m, surface area = 56.44 km^2) located in Chatham County, North Carolina, which serves as a source of drinking water to neighboring areas. It also provides recreation and other services in the Triangle region. However, it has been consistently classified as eutrophic since its dedication in 1983. So, as part of the Jordan Lake

Nutrient Management Study, a water quality model was developed to carryout eutrophication studies. It is commonly referred to as Jordan Lake Reservoir Model (Del Giudice et al., 2019). For modeling and analysis purposes, the reservoir was divided into four segments, north to south (upstream to downstream), based on locations of flow constriction. In the model, P release fluxes were determined using a mass-balance approach, with rates derived by integrating prior information (from literature review) with calibration to historical surface-water data through Bayesian inference.

Modeled phosphorus release fluxes from the sediments of Jordan Lake varied across seasons (Figure 1). Here, seasons are defined as: winter – January to March, spring – April to June, summer – July to September, and fall – October to December. Note that July, August, and September represent the warmest three months for the reservoir. As expected, there is a large variation in sediment P release fluxes with temperature. While in winter, the average sediment P release flux in Jordan Lake was 0.11 g/m^2/month, the same rose to 0.53 g/m^2/month during the summer (Table 3). Fall and spring had intermediate values with higher flux in spring due to higher temperature. The calibrated temperature adjustment factor (θ) was about 1.1. It should be noted that the bottom waters in Jordan Lake turn anoxic in the warm season (which is reflected in the calibrated θ). The estimated sediment P release fluxes in winter and summer are generally consistent with literature values (Tables 1 and 2) under aerobic and anaerobic conditions, respectively. The overall temporal trend was similar for each segment, but downstream Segment 4 had somewhat higher P releases (Table 3). In the model, this was due to a high rate of P loading (from Haw River, which enters Segment 4) relative to the segment area.

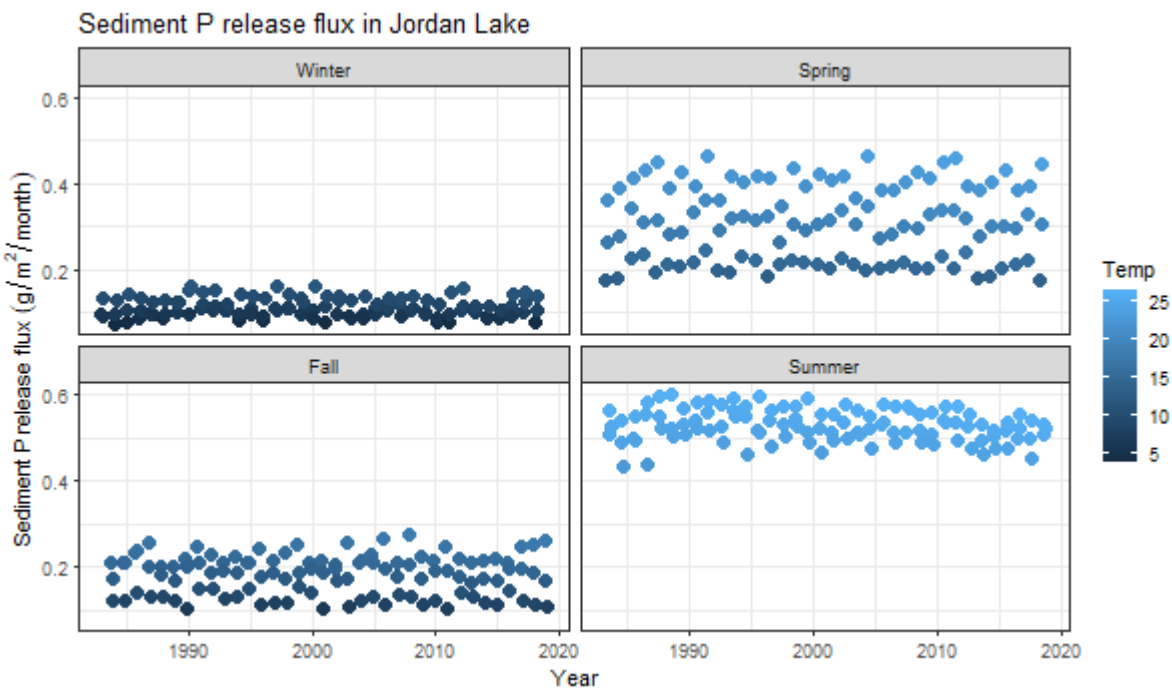

Figure 1. Seasonal sediment P release flux estimated in Jordan Lake using Jordan Lake Reservoir Model

Table 3. Model-estimated average sediment P release fluxes in Jordan Lake in different seasons and segments

Season	Average internal P release flux ($g/m^2/month$)				
	Segment 1	**Segment 2**	**Segment 3**	**Segment 4**	**Overall**
Winter	0.12	0.11	0.10	0.17	0.11
Spring	0.32	0.29	0.28	0.46	0.31
Summer	0.55	0.49	0.47	0.78	0.53
Fall	0.19	0.17	0.16	0.27	0.18

A sediment core study was carried out by Zeller and Alperin (2021) in Jordan Lake during 2017-2018. The sediment cores were collected from the southern end of Segment 1 and incubated at 19-20° C. This study reported an average sediment P release flux of 7.0 μmol $P/m^2/day$, which is equivalent to 0.007 $g/m^2/month$ (markedly lower than the typical literature values from Tables 1 and 2). However, the average sediment P release flux under anoxic conditions was reported as 236 μmol $P/m^2/day$, which is equivalent to 0.22 $g/m^2/month$. This value is within range of anaerobic sediment P release fluxes in other sediment core studies (Table 1) but lower than the *in-situ* studies (Table 2). The anaerobic release flux is also comparable to typical release fluxes from the Jordan Lake Reservoir Model for spring (Figure 1) when reservoir water temperatures were most similar to the core incubation temperatures (spring and fall).

Sediment P release in Falls Lake

Formed by impoundment of Neuse River, Falls Lake (mean depth = 3.2 m, surface area = 50.2 km^2) is another important reservoir in central North Carolina (Lin and Li 2011). Like Jordan Lake, this reservoir has suffered from eutrophication since its impoundment. So, to understand the contribution of internal nutrient loading and aid modelling efforts, different sediment studies were carried out in the Falls Lake.

In 2011, a nutrient response model was developed to understand the impact of different levels of nutrient loading on the Falls Lake (Lin and Li, 2011). To support model calibration and validation, sampling was carried out by NC Division of Water Quality (DWQ) during 2005-2007. The sampling strategy also included estimation of sediment P release flux from 2 locations, but no sediment P release flux was detected. Hence, calibrated constant values of 0.0023 $g/m^2/day$ (0.07 $g/m^2/month$) and 0.001 $g/m^2/day$ (0.03 $g/m^2/month$) were selected for the years 2005 and 2006, respectively.

In 2015, another sediment study was conducted for Upper Neuse River Basin Association (UNRBA) to understand the role of internal nutrient loading in Falls Lake (Alperin, 2018). The diffusive flux method was employed to evaluate the potential release of P from the sediments during the summer of 2015. Based on this study, the mean P release flux from the sediments was estimated to be 0.004 $mmol/m^2/day$, which is equivalent to 0.004 $g/m^2/month$. This is considerably lower than the typical literature values (Tables 1 and 2).

A third sediment study was carried out by US EPA Region 4 Science and Ecosystem Support Division (SESD), the results were startlingly different (Flexner, 2019). The study was carried out in the summer of 2018 using box chambers to measure *in-situ* sediment P release flux at three

locations. This study provided interesting insights. In one of the locations where aerobic conditions were typically observed, there was net sediment P uptake (mean = -0.25 g/m^2/month) instead of sediment P release. But, in two locations where anaerobic condition normally prevailed, average sediment P release fluxes were 0.27 g/m^2/month (TP; TDP = 0.18 g/m^2/month) and 0.62 g/m^2/month (TP; TDP = 0.58 g/m^2/month). These values are much higher than those in the 2015 study and more consistent with the literature review (Tables 1 and 2). The mean value of anaerobic sediment P release (0.44 g/m^2/month) is comparable to the average sediment P release fluxes modeled in the summer season of Jordan Lake (Table 3) when the hypolimnetic water is expected to be in anaerobic condition.

Conclusion

Based on the literature review carried out in this memorandum, average sediment P release fluxes under aerobic conditions range from 0 to 0.15 g/m^2/month, whereas under anaerobic conditions, fluxes range from 0 to 1.2 g/m^2/month. These values are generally consistent with previous reviews, including a range of 0–1.58 g/m^2/month for lakes worldwide (Nürnberg, 1988) and -0.82–1.64 g/m^2/month for Canadian lakes (Orihel et al., 2017). The modeled P release fluxes for Jordan Lake (varying from 0.10–0.78 g/m^2/month depending on season and segment) are also consistent with these literature ranges. However, there is wide variation in the reported P release fluxes for Falls Lake. Multiple factors control sediment P release, and their complex inter-relationships complicate attempts to generalize the flux rates and mechanisms for a given geographic region. Therefore, to get a better estimate of sediment P release for a particular lake or reservoir, it is preferable to carry out dedicated sediment experiments and modeling analyses for that water body.

References

Alperin, M. (2018). Falls Lake sediment study (tech. rep.). Upper Neuse River Basin Association. https://www.unrba.org/sites/default/files/Alperin%20Sediment%20Study%2011719.pdf

Anderson, H. S., Johengen, T. H., Godwin, C. M., Purcell, H., Alsip, P. J., Ruberg, S. A., & Mason, L. A. (2021). Continuous in-situ nutrient analyzers pinpoint the onset and rate of internal p loading under anoxia in Lake Erie's Central Basin. ACS ES&T Water.

Carter, L. D., & Dzialowski, A. R. (2012). Predicting sediment phosphorus release rates using landuse and water-quality data. Freshwater Science, 31(4), 1214–1222. https://doi.org/10.1899/11-177.1

Chapra, S. C. (2008). Surface Water-Quality Modeling. Waveland Press, Inc.

Chapra, S. C., & Canale, R. P. (1991). Long-term phenomenological model of phosphorus and oxygen for stratified lakes. Water Research, 25(6), 707–715. https://doi.org/10.1016/0043-1354(91)90046-S

Cooke, G. D., Welch, E. B., & Jones, J. R. (2011). Eutrophication of Tenkiller reservoir, Oklahoma, from nonpoint agricultural runoff. Lake and Reservoir Management, 27(3), 256–270. https://doi.org/10.1080/07438141.2011.607552

Del Giudice, D., Aupperle, M., Arumugam, S., & Obenour, D. R. (2019). Jordan Lake Watershed Model report (tech. rep. December). https://nutrients.web.unc.edu/wp-content/uploads/sites/19393/2019/12/Reservoir-Model-NCSU.pdf

Flexner, M. (2019). Falls Lake Nutrient Exchange & Sediment Oxygen Demand (SOD) Study Final Project Report, Version 2 (tech. rep.). Field Services Branch, Science & Ecosystem Support Division, USEPA - Region 4.

Gächter, R., & Wehrli, B. (1998). Ten years of artificial mixing and oxygenation: No effect on the internal phosphorus loading of two eutrophic lakes. Environmental Science & Technology, 32(23), 3659–3665. https://doi.org/10.1021/es980418l

Gibbons, K. J., & Bridgeman, T. B. (2020). Effect of temperature on phosphorus flux from anoxic western Lake Erie sediments. Water Research, 182, 116022. https://doi.org/10.1016/j.watres.2020.116022

Haggard, B. E., Moore Jr., P. A., & DeLaune, P. B. (2005). Phosphorus flux from bottom sediments in Lake Eucha, Oklahoma. Journal of Environmental Quality, 34(2), 724–728. https://doi.org/10.2134/jeq2005.0724

Havens, K. E., Carrick, H. J., Lowe, E. F., & Coveney, M. F. (1999). Contrasting relationships between nutrients, chlorophyll a and secchi transparency in two shallow subtropical lakes: Lakes Okeechobee and Apopka (Florida, USA). Lake and Reservoir Management, 15(4), 298–309. https://doi.org/10.1080/07438149909354125

Hemond, H. F., & Lin, K. (2010). Nitrate suppresses internal phosphorus loading in a eutrophic lake. Water Research, 44(12), 3645–3650. https://doi.org/10.1016/j.watres.2010.04.018

Holdren, G. C., & Armstrong, D. E. (1980). Factors Affecting Phosphorus Release From Intact Lake Sediment Cores. Environmental Science and Technology, 14(1), 79–87. https://doi.org/10.1021/es60161a014

Hupfer, M., & Lewandowski, J. (2008). Oxygen controls the phosphorus release from lake sediments – a long-lasting paradigm in limnology. International Review of Hydrobiology, 93(4-5), 415–432. https://doi.org/10.1002/iroh.200711054

Jacoby, J., Lynch, D., Welch, E., & Perkins, M. (1982). Internal phosphorus loading in a shallow eutrophic lake. Water Research, 16(6), 911–919. https://doi.org/10.1016/0043-1354(82)90022-7

James, W. F. (2017). Phosphorus binding dynamics in the aluminum floc layer of Half Moon Lake, Wisconsin. Lake and Reservoir Management, 33(2), 130–142. https://doi.org/10.1080/10402381.2017.1287789

James, W. F., Barko, J. W., & Eakin, H. L. (1995). Internal phosphorus loading in Lake Pepin, Upper Mississippi River. Journal of Freshwater Ecology, 10(3), 269–276. https://doi.org/10.1080/02705060.1995.9663446

James, W. F., Barko, J. W., Eakin, H. L., & Helsel, D. R. (2000). Distribution of sediment phosphorus pools and fluxes in relation to alum treatment. JAWRA Journal of the American Water Resources Association, 36(3), 647–656. https://doi.org/10.1111/j.1752-1688.2000.tb04294.x

Jensen, J. P., Pedersen, A. R., Jeppesen, E., & Søndergaard, M. (2006). An empirical model describing the seasonal dynamics of phosphorus in 16 shallow eutrophic lakes after external loading reduction. Limnology and Oceanography, 51(1part2), 791–800. https://doi.org/10.4319/lo.2006.51.1_part_2.0791

Larsen, D. P., Schults, D. W., & Malueg, K. W. (1981). Summer internal phosphorus supplies in Shagawa Lake, Minnesota. Limnology and Oceanography, 26(4), 740–753. http://www.jstor.org/stable/2836039

Le Moal, M., Gascuel-Odoux, C., Ménesguen, A., Souchon, Y., Étrillard, C., Levain, A., Moatar, F., Pannard, A., Souchu, P., Lefebvre, A., & Pinay, G. (2019). Eutrophication: A new wine in an old bottle? Science of the Total Environment, 651, 1–11. https://doi.org/10.1016/j.scitotenv.2018.09.139

Lin, J., & Li, J. (2011). Nutrient response modeling in Falls of the Neuse Reservoir. Environmental Management, 47(3), 398–409. https://doi.org/10.1007/s00267-011-9617-4

Matisoff, G., Kaltenberg, E. M., Steely, R. L., Hummel, S. K., Seo, J., Gibbons, K. J., Bridgeman, T. B., Seo, Y., Behbahani, M., James, W. F., Johnson, L. T., Doan, P., Dittrich, M., Evans, M. A., & Chaffin, J. D. (2016). Internal loading of phosphorus in western Lake Erie. Journal of Great Lakes Research, 42(4), 775–788. https://doi.org/10.1016/j.jglr.2016.04.004

Moore, P. A., Reddy, K. R., & Fisher, M. M. (1998). Phosphorus Flux between Sediment and Overlying Water in Lake Okeechobee, Florida: Spatial and Temporal Variations. Journal

of Environmental Quality, 27(6), 1428–1439. https://doi.org/10.2134/jeq1998.00472425002700060020x

Moore Jr., P. A., Reddy, K. R., & Graetz, D. (1991). Phosphorus geochemistry in the sediment water column of a hypereutrophic lake. Journal of Environmental Quality, 20(4), 869–875. https://doi.org/10.2134/jeq1991.00472425002000040027x

Mortimer, C. H. (1942). The exchange of dissolved substances between mud and water in lakes. Journal of Ecology, 30(1), 147–201. http://www.jstor.org/stable/2256691

Nürnberg, G. K. (1988). Prediction of phosphorus release rates from total and reductant-soluble phosphorus in anoxic lake sediments. Canadian Journal of Fisheries and Aquatic Sciences, 45(3), 453–462. https://doi.org/10.1139/f88-054

Olila, O. G., & Reddy, K. R. (1995). Influence of ph on phosphorus retention in oxidized lake sediments. Soil Science Society of America Journal, 59(3), 946–959. https://doi.org/10.2136/sssaj1995.03615995005900030046x

Orihel, D. M., Baulch, H. M., Casson, N. J., North, R. L., Parsons, C. T., Seckar, D. C., & Venkiteswaran, J. J. (2017). Internal phosphorus loading in canadian fresh waters: A critical review and data analysis. Canadian Journal of Fisheries and Aquatic Sciences, 74(12), 2005–2029. https://doi.org/10.1139/cjfas-2016-0500

Pollman, C. D., & James, R. T. (2011). A simple model of internal loading of phosphorus in Lake Okeechobee. Lake and Reservoir Management, 27(1), 15–27. https://doi.org/10.1080/07438141.2010.542877

Reddy, K. R., Fisher, M. M., & Ivanoff, D. (1996). Resuspension and diffusive flux of nitrogen and phosphorus in a hypereutrophic lake. Journal of Environmental Quality, 25(2), 363–371. https://doi.org/10.2134/jeq1996.00472425002500020022x

Schindler, D. W., Carpenter, S. R., Chapra, S. C., Hecky, R. E., & Orihel, D. M. (2016). Reducing phosphorus to curb lake eutrophication is a success. Environmental Science & Technology, 50(17), 8923–8929. https://doi.org/10.1021/acs.est.6b02204

Sondergaard, M., Jensen, P. J., & Jeppesen, E. (2001). Retention and internal loading of phosphorus in shallow, eutrophic lakes. TheScientificWorldJournal, 1, 427–442. https://doi.org/10.1100/tsw.2001.72.

Zeller, M. A., & Alperin, M. J. (2021). The efficacy of phoslock® in reducing internal phosphate loading varies with bottom water oxygenation. Water Research X, 11, 100095. https://doi.org/10.1016/j.wroa.2021.100095

Appendix A: Lake Segmentation Memorandum

From: Daniel Obenour, PhD, NC State University

To: Forrest Westall, PE, UNRBA

Date: 6 Oct 2020

Re: Falls Lake "WARMF Lake" Model Segmentation

Background:

Some water quality models represent waterbodies as a series of continuously stirred tank reactors (CSTRs). Reservoir segments are well represented using CSTRs when the segments are isolated from each other (e.g., due to constrictions) and when the rate of diffusive transport greatly exceeds the rate of advective transport within each segment (i.e., Peclet <0.1; Chapra, 2008). Waterbodies can also be represented as plug flow reactors (PFRs), particularly when advective transport greatly exceeds diffusive transport (i.e., Pelcet >10, as in some streams). In practice, a PFR can be represented by a large number of CSTRs in series. A comparison of contaminant decay in a waterbody treated alternatively as a PFR versus a series of 5 CSTRs is shown below. Note that the PFR representation results in greater contaminant reduction, all else being equal, highlighting a substantive difference between these two approaches.

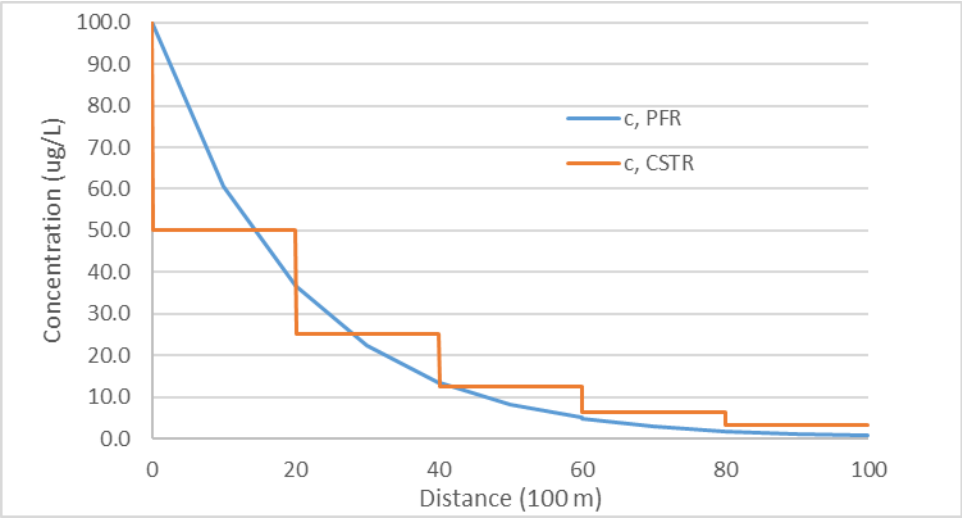

Figure 1: Concentration profile for a waterbody modeled as a PFR versus a series of 5 CSTRs. In both cases, the hypothetical substance is assumed to decay at a rate of 0.05/100 m.

The morphology of Falls Lake suggests potential modeling representations. The upstream portion of Falls Lake (above Creedmor Road) can be divided into wide segments separated by obvious constrictions (e.g., at road causeways), such that a CSTR representation appears appropriate for these segments (this could be verified mathematically). The downstream portion

of Falls Lake (i.e., below Creedmor Road) is relatively narrow, such that advective transport may exceed diffusive transport, indicating a PFR (or large number of CSTRs in series) representation may be more appropriate. However, if nutrient concentrations do not vary as much in the lower segments, using a smaller number of CSTRs may not lead to appreciable model error.

Discussion items:

1. Add additional segment to the lake model, splitting the current segment that extends from I-85 to the Rolling View pinch point. (Agree or Disagree)

   Since the proposed split would presumably occur at the Cheek Road causeway, which is a major constriction point, adding an additional segment will improve the mechanistic realism of the model

2. Perform calibration to data at the downstream end of each segment, instead of the segment average. (Agree or Disagree)

   In reality, reservoirs do not behave as perfect CSTRs or PFRs, but rather somewhere in between. Thus, both calibration approaches represent a compromise. Calibrating to segment mean/midpoints is more consistent with the mathematical representation of the reservoir as a series of CSTRs, as proposed by "WARMF Lake". Calibrating to segment mean/midpoints would be more critical if the flow can reverse (as in Jordan Lake). On the other hand, given a consistent flow direction (as in Falls Lake), calibration to segment end points can result in (slightly) more accurate loading inputs to downstream segments. Given the small changes in observed concentrations (e.g., nutrients) among adjacent segments (based on the currently proposed segmentation), either approach is expected to be a workable representation of the system.

References:

Chapra, S. C. (2008). Surface water-quality modeling. Waveland press.

Appendix B: Flow Balance Memorandum

From: Daniel Obenour, PhD, NC State University

To: Forrest Westall, PE, UNRBA

Date: 1 January 2021

Re: Falls Lake Model Flow Balance Question.

Background:

Data are generally available for the major components of the Falls Lake water budget (e.g., inflows, dam discharge, over-lake precipitation, evaporation). Balancing the water budget is critical to ensuring realistic model simulations for water quality. However, because the available datasets are imperfect, the water budget will not balance without adjustment. To provide this adjustment, "balance flows" will be added to the model.

Based on recent data analysis provided by UNRBA, the magnitudes of the required balance flows are not correlated with groundwater levels (from a nearby observation well), suggesting that groundwater should not be used to balance the reservoir's water budget.

In a similar modeling study of High Rock Lake, LOESS (LOcally Estimated Scatterplot Smoothing, Cleveland & Devlin, 1988) was applied to smooth the required daily balance flows to enforce "approximate consistency between observed and simulated water surface elevations without imposing sudden shocks on the system" (NC DWR, 2016). In this case, they applied LOESS with an alpha value of 0.1 to data covering an approximately 5.25-year period. Roughly, based on visual examination (Figure 3-2, NC DWR, 2016), this reduced the standard deviation of the balance flows by around one order of magnitude (90%).

LOESS Smoothing:

LOESS makes predictions based on locally-fitted regressions (often second-order polynomials) developed from data within a moving window defined by parameter alpha (a.k.a., the "span" or "smoothing parameter"). Alpha is the fraction of the overall dataset to be included in each local regression. Thus, in the case of the High Rock Lake model, the window is about 192 days wide. Within this window, data are weighted, often with a tricubic function (e.g., R Core Team, 2013).

The span, alpha, is highly influential. Figure 1 shows a pseudo-dataset with LOESS with an alpha of 0.75 (a default value, R Core Team, 2013) and LOESS with an alpha set to 0.10. In this case, with 100 days total, the windows for alphas of 0.75 and 0.10 correspond to 75 and 10 days, respectively.

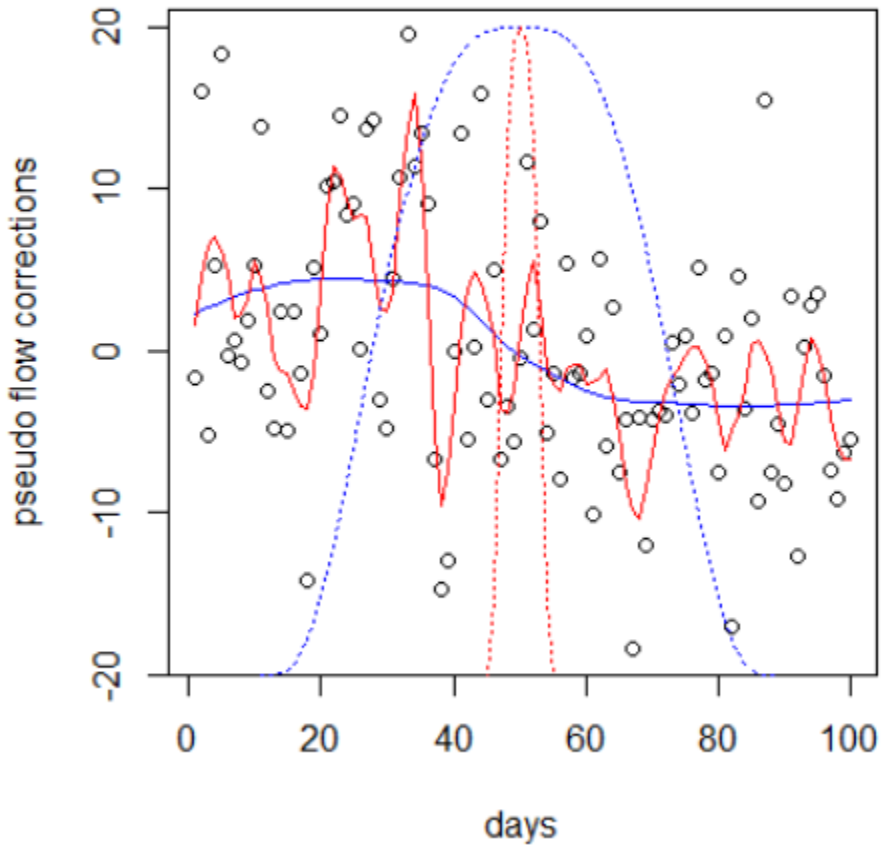

Figure 1: Pseudo-dataset of flow corrections (i.e., "balance flows") along with LOESS smoothing with alpha=0.75 (blue solid line) and alpha=0.10 (red solid line). Dashed lines illustrate the shapes of the corresponding tricubic weighting functions when making a prediction for day=50.

Discussion items:

3. Set the flow additions and withdrawals proportional to the drainage areas of 17 tributaries to Falls Lake at the EFDC cell adjacent to the location of the tributary inflow. (Agree or Disagree)

   Agree. As discussed during the meeting on 30 November, tributary inflows have the largest uncertainties. This is for multiple reasons, including uncertainties in meteorological data (especially precipitation over the watershed) and uncertainties in the watershed model used to generate the flows. As mentioned before, groundwater levels do not correlate with balance flows. Water withdrawals and dam discharges are expected to be measured with relatively high accuracy. Other components of the water balance, such as over-lake precipitation and evaporation, also have uncertainty, but are probably too small to account

for the required balance flows. Thus, distributing the balance flow among the reservoir tributaries should be the most straightforward defensible approach.

4. Apply flow balance smoothing using locally weighted scatterplot smoothing (LOESS). (Agree or Disagree)

   Agree. Providing some degree of smoothing makes sense, considering uncertainties and lags in the timing of high/low flow events. Lags can be related to watershed and reservoir travel times. These travel times may be represented within the watershed and reservoir modeling, but with uncertainties (particularly for the watershed model). In addition, some smoothing may be required to prevent reservoir modeling shocks/instabilities, as suggested by the DWR/Tetra Tech report (NC DWR, 2016).

5. Suggestions for the smoothing factor, alpha. (Provide input)

   I am not aware of any standard smoothing protocols for use in watershed or water quality modeling. However, I think it is better to focus on the appropriate length of days for the smoothing window rather than some fraction of the overall dataset (alpha). If we can agree on an appropriate number of days, then alpha can be simply back-calculated assuming we have continuous daily flow data (i.e., alpha=[desired window in days]/[total period of record in days]). I would suggest determining a smoothing factor based on a comparison of USGS flow records to corresponding watershed model simulation outputs, particularly for large watersheds. For example, the temporal offsets between simulated and observed flow peaks could be used as a basis for determining the desired window span (days). I think a very large window span (e.g., 192 days) may be undesirable, especially if it removes variability in flow (and potentially load) that should be retained in the overall modeling framework to account for the full range of variability in reservoir water quality. When considering this need, one could assess how well the hydrologic modeling output already captures the natural range and standard deviation of observed USGS flow data.

References:

Cleveland, W. S., & Devlin, S. J. (1988). *Locally weighted regression: an approach to regression analysis by local fitting*. Journal of the American statistical association, 83(403), 596-610.

NC DWR (2016). *High Rock Lake Hydrodynamic and Nutrient Response Models*. North Carolina Division of Water Resources. https://files.nc.gov/ncdeq/Water%20Quality/Planning/TMDL/Internal%20files/Final_HighRockLakeModel_Mar2015_revFeb2016_revAug2016_revOct2016.2.pdf

R Core Team. (2013). R: A language and environment for statistical computing. R Foundation for Statistical Computing.